New Discrete Basis for Nuclear Structure Studies

M.V. Stoitsov,[1,2] W. Nazarewicz,[3–5] and S. Pittel,[6]
[1]*Institute of Nuclear Research and Nuclear Energy, Bulgarian Academy of Sciences Sofia-1784, Bulgaria*
[2]*Joint Institute for Heavy Ion Research, Oak Ridge, Tennessee 37831*
[3]*Department of Physics, University of Tennessee, Knoxville, Tennessee 37996*
[4]*Physics Division, Oak Ridge National Laboratory, Oak Ridge, Tennessee 37831*
[5]*Institute of Theoretical Physics, University of Warsaw, ul. Hoża 69, PL-00-681 Warsaw, Poland*
[6]*Bartol Research Institute, University of Delaware, Newark, Delaware 19716*
(February 9, 2008)

Abstract

A complete discrete set of spherical single-particle wave functions for studies of weakly-bound many-body systems is proposed. The new basis is obtained by means of a local-scale point transformation of the spherical harmonic oscillator wave functions. Unlike the harmonic oscillator states, the new wave functions decay exponentially at large distances. Using the new basis, characteristics of weakly-bound orbitals are analyzed and the ground state properties of some spherical doubly-magic nuclei are studied. The basis of the transformed harmonic oscillator is a significant improvement over the harmonic oscillator basis, especially in studies of exotic nuclei where the coupling to the particle continuum is important.

PACS number(s): 21.10.Pc, 21.60.Cs, 21.60.Jz, 71.15.Mb

I. INTRODUCTION

Understanding the nature of exotic nuclei with extreme isospin values is one of the most exciting challenges of current nuclear structure physics. Thanks to developments in radioactive ion beam instrumentation, we are in the process of exploring the very limits of nuclear binding, namely the regions of the periodic chart in the neighborhood of the particle drip lines. Several new structural features arise in the description of nuclei near the drip lines. Firstly, such nuclei exhibit very weak binding, which leads to extended spatial distributions. Secondly, the particle continuum plays a critical role in a description of the properties of these nuclei. Unlike more stable nuclei closer to the valley of beta stability, a proper theoretical description of weakly-bound systems (such as halo nuclei) requires a very careful treatment of the asymptotic part of the nucleonic density.

The correct treatment of the particle continuum and near-threshold (e.g. halo) states poses a significant theoretical challenge. One possible way of tackling this problem is by means of the continuum shell model (CSM), in which the basis consists of both bound and unbound states, e.g., the eigenvectors of some finite shell-model potential [1–7]. An alternative approach is to discretize the continuum by means of Sturmian function expansions or resonant state expansions. Sturmian functions form a discrete set of states which behave asymptotically as outgoing waves; they have been used as a basis in the solution of scattering equations, including various applications of the CSM [2,8,9]. The Gamow (Berggren) states are the eigenstates of the time-independent Schrödinger equation with complex eigenvalues [10–12]; they have been applied to many problems involving an unbound spectrum [13–15]. Another possibility is to employ the canonical Hartree-Fock-Bogolyubov (HFB) basis of the independent-quasiparticle Hamiltonian [16,17]. The canonical states, i.e., the eigenstates of the one-body density matrix, form a complete localized basis with proper one-body asymptotics. Unfortunately, in order to find the canonical basis, the self-consistent one-body density matrix must be known, and this is not always possible. Finally, the particle continuum can be discretized by placing the nucleus inside a very large box. Since the properties of the nucleus itself must not depend on the box size, one has to subtract the contribution from the free-gas states that are introduced [18–20]. The coordinate-space HFB [16,17,21,22] and relativistic Hartree-Bogolyubov (RHB) [23] methods are based on this principle.

One of the most important tools of nuclear structure physics is the harmonic oscillator (HO) potential. The simple analytic structure of HO wave functions greatly simplifies shell-model studies [24–26]. Since the HO wave functions form a complete *discrete* set, they typically serve as the single-particle basis of choice in microscopic many-body calculations. Another useful feature of HO states is that they are all spatially localized, so that the resulting densities and currents are localized as well. The disadvantage of HO wave functions is that, because of their gaussian asymptotics, they cannot describe the falloff of nuclear density distributions near the nuclear surface and beyond. To get the falloff correct, it is essential to mix HO basis states. This is a serious problem when dealing with weakly-bound nuclei, where the density distributions fall off very slowly and the bases required are extremely large and thus very difficult to handle. Hence, the HO basis is not particularly useful when dealing with weakly-bound nuclei.

It is desirable, therefore, to have an alternative to HO wave functions for use in nuclear

structure studies. Ideally, the new basis should preserve as many of the advantageous features of HO wave functions as possible, but, at the same time, it should have an improved asymptotic behavior. In this work, we consider a new spherical single-particle basis, obtained through the application of a general local-scaling point transformation to harmonic oscillator wave functions. This approach was originally developed by Petkov and Stoitsov, and is described in detail in Ref. [27]. In this study, we pay particular attention to the asymptotic form of the resulting transformed HO wave functions, developing the method so as to guarantee an appropriate exponential falloff. This makes the new basis especially useful in the description of weakly-bound nuclear systems.

The paper is organized as follows. Section II briefly reviews the method of Petkov and Stoitsov, and introduces the transformed HO basis. Stability tests of the new basis, when applied to weakly-bound orbitals, are contained in Sec. III. In Sec. IV, we use the new basis in variational calculations based on the density functional theory. Finally, Sec. V summarizes the principal conclusions of the work and spells out some issues for future consideration.

II. TRANSFORMED OSCILLATOR BASIS

A. Local-scale point transformations

The key ingredient in the construction of our new basis is a coordinate transformation based on the local-scale transformation method [27]. A local-scaling point transformation (LST) replaces the original coordinate $\mathbf{r}$ by a new coordinate $\mathbf{r}' = \mathbf{f}(\mathbf{r}) \equiv \hat{\mathbf{r}} f(\mathbf{r})$. The new coordinate is in the same direction as $\mathbf{r}$, but has a new magnitude $r' = f(\mathbf{r})$, depending on a scalar function $f(\mathbf{r})$ (called the LST function). It is assumed that $f(\mathbf{r})$ is an increasing function of r and $f(\mathbf{0})$=0. The set of invertible transformations of this type forms a LST group.

Given a model A-particle wave function $\bar{\Psi}(\mathbf{r}_1, \mathbf{r}_2, ..., \mathbf{r}_A)$, the LST transforms it into a new wave function

$$\Psi_f(\mathbf{r}_1, \mathbf{r}_2, ..., \mathbf{r}_A) = \left[\prod_{i=1}^{A} \frac{f^2(\mathbf{r}_i)}{r_i^2} \frac{\partial f(\mathbf{r}_i)}{\partial r_i}\right]^{1/2} \bar{\Psi}(\mathbf{f}(\mathbf{r}_1), \mathbf{f}(\mathbf{r}_2), ..., \mathbf{f}(\mathbf{r}_A)). \tag{1}$$

Assuming that the model wave function is normalized to unity,

$$\langle \bar{\Psi} | \bar{\Psi} \rangle = 1, \tag{2}$$

the LST wave function $\Psi_f(\mathbf{r}_1, \mathbf{r}_2, ..., \mathbf{r}_A)$ will also be normalized to unity, regardless of the choice of $f(\mathbf{r})$.

The local one-body density corresponding to an A-body wave function Ψ is

$$\rho(\mathbf{r}) = A \int |\Psi(\mathbf{r}, \mathbf{r}_2, ..., \mathbf{r}_A)|^2 d\mathbf{r}_2, ..., d\mathbf{r}_A \ . \tag{3}$$

It then follows from (1) that there exists a simple relation between the local density $\rho_f(\mathbf{r})$ associated with the LST function Ψ_f and the model local density $\bar{\rho}(\mathbf{r})$ corresponding to the model function $\bar{\Psi}$:

$$\rho_f(\mathbf{r}) = \frac{f^2(\mathbf{r})}{r^2}\frac{\partial f(\mathbf{r})}{\partial r}\bar{\rho}(\mathbf{f}(\mathbf{r})) \ . \tag{4}$$

The relation (4) is particularly useful when the density $\rho_f(\mathbf{r})$ is known (or at least approximately known). Given a model wave function, Eq. (4) becomes a first-order nonlinear differential equation for the LST function f. For a spherically symmetric system, ρ_f, $\bar{\rho}$, and f depend only on r=$|\mathbf{r}|$, and Eq. (4) can be reduced to the nonlinear algebraic equation

$$\int_0^r \rho_f(u)u^2du = \int_0^{f(r)} \bar{\rho}(u)u^2du \ , \tag{5}$$

which can be solved subject to the boundary condition $f(0) = 0$. Such an approach was pursued in a series of works [28–30] based on the energy density functional method. A review of the density functional theory based on the LST can be found in the monograph [31].

In the context of shell-model or mean-field applications, the particularly interesting case is when the model function is a Slater determinant,

$$\bar{\Psi}(\mathbf{r}_1, \mathbf{r}_2, ..., \mathbf{r}_A) = \frac{1}{\sqrt{A!}} \det|\bar{\psi}_i(\mathbf{r}_j)| \ , \tag{6}$$

built from a complete set of model single-particle wave functions $\bar{\psi}_i(\mathbf{r})$. Due to the unitarity of transformation (1), the LST wave function retains the structure of a Slater determinant,

$$\Psi_f(\mathbf{r}_1, \mathbf{r}_2, ..., \mathbf{r}_A) = \frac{1}{\sqrt{A!}} \det|\psi_i(\mathbf{r}_j)| \ , \tag{7}$$

but with new single-particle wave functions

$$\psi_i(\mathbf{r}) = \left[\frac{f^2(\mathbf{r})}{r^2}\frac{\partial f(\mathbf{r})}{\partial r}\right]^{1/2} \bar{\psi}_i(\mathbf{f}(\mathbf{r})) \ . \tag{8}$$

These functions, in the following referred to as the LST basis, form a complete set of single-particle states.

B. Transformed harmonic oscillator basis

Having in mind the numerous advantages of the HO basis, we choose for the model single-particle wave functions the eigenfunctions of a HO potential. Since in this work we consider spherically symmetric systems only, the angular part of the single-particle wave function is not affected by the LST transformation. The radial HO wave functions $R^{\rm HO}_{nl}(r)$ are characterized by one external parameter, namely the oscillator length $a_{\rm osc} = \sqrt{\hbar/M\omega}$. The LST basis associated with HO model wave functions will be referred to throughout the remainder of this paper as the transformed harmonic oscillator (THO) basis. The states in this basis are given by Eq. (8):

$$R^{\rm THO}_{nl}(r) = \left[\frac{f^2(r)}{r^2}\frac{df(r)}{dr}\right]^{1/2} R^{\rm HO}_{nl}(f(r)). \tag{9}$$

Up to this point, the LST function has not been defined. Ideally, we would like to parametrize $f(r)$ in as simple manner as possible consistent with the requirement that it reproduces the generic features of the local density ρ_f at small and large distances r. Of course, the actual behavior of ρ_f is affected by nuclear shell effects. Therefore, we concentrate on the average behavior of $\rho_f(r)$ only.

In the nuclear interior, the average local density varies rather weakly with r. Due to the effects of Coulomb repulsion, the proton charge density is expected to exhibit a central depression [32]. Consequently, at low values of r, we assume the following ansatz:

$$\rho(r) \approx \rho_0 + cr^2. \tag{10}$$

Eq. (5) can then be cast into a fifth-order polynomial equation for the LST function $f(r)$ at small r. To further simplify the problem, we assume that the model density $\tilde{\rho}(r)$ is constant in the inner region. In this limit, the LST function assumes the simple form

$$f(r) = r(a + br^2)^{1/3} \ , \tag{11}$$

where a and b are parameters still to be determined.

For large values of r, i.e., outside the nucleus, the average LST density should decay exponentially. Hence,

$$\rho(r) \approx \rho(R) \exp\left(\frac{R-r}{\tilde{a}}\right) \ , \tag{12}$$

where R is a characteristic LST radius that is significantly greater than the nuclear radius and $\tilde{a}$ is the LST diffuseness parameter. In contrast, the model density based on HO states exhibits a gaussian asymptotic behavior. Using Eq. (5), we obtain an approximate expression for $f(r)$ at large distances,

$$f(r) = \sqrt{\frac{d_{-2}}{r^2} + \frac{d_{-1}}{r} + d_0 + d\ln r + d_1 r} \ , \tag{13}$$

where d_{-2}, d_{-1}, d_0, d_1, and d are parameters. Asymptotically, the linear term in the expansion (13) takes over and $f(r \to \infty) \sim r^{1/2}$, as it should.

The parameters $\{d_{-2}, d_{-1}, d_1, d_0, d\}$ can be determined by the requirement that $f(r)$ and its first, second, third, and fourth derivatives are continuous at the point R. We are then left with only three independent parameters $\{a, b, R\}$ in the LST function $f(r)$, which can be chosen to optimize the THO basis for the physics problem of interest. In practical calculations, we assume that $a, b \geq 0$, thereby ensuring that $f(r)$ is a monotonically increasing function of r.

The ansatz (11)-(13) for the LST function guarantees that all the THO states (9) are spatially localized and decay exponentially at large distances. The THO functions are continuous up to their fourth derivatives. The HO length is absorbed into the coefficients a and b, and does not appear as an additional parameter. It should be stressed here that the parametrization of $f(r)$ assumed in our work reflects our desire to keep it as simple and practical as possible. Although, as will be demonstrated in the following sections, this three-parameter form of the LST function performs very well in actual calculations, other choices are possible and could prove useful (or even essential) in other applications.

III. APPLICATION OF THE THO BASIS TO WEAKLY-BOUND STATES

On the neutron-rich side of the valley of stability, there appear loosely-bound few-body systems called neutron halo nuclei (see Refs. [33–36] for reviews). In these nuclei, weak neutron binding implies large spatial dimensions and the existence of the halo (i.e., a dramatic excess of neutrons at large distances). Theoretically, the weak binding and the corresponding proximity to the particle continuum, together with the need for explicit treatment of few-body dynamics, makes the subject of halos both extremely interesting and difficult.

In this section, we apply the THO basis to weakly-bound single-particle states to assess its potential usefulness in the description of nuclei far from stability and, in particular, halo nuclei. We focus on spherical single-particle states and assume that they come from a finite square well (SQW) potential with radius R_0 and depth $-V_0$. We concentrate on ℓ=0 orbitals, since they are the best candidates for halos [37,38].

More specifically, we carry out a diagonalization of the SQW Hamiltonian within a truncated THO single-particle basis and compare the results that emerge with those of the exact SQW solutions. For the sake of comparison, we also carry out calculations in the analogous truncated HO basis. All calculations are carried out for a fixed radius R_0=7.11 fm of the SQW potential and under the assumption that the most weakly-bound ℓ=0 state is the $3s$. To simulate scenarios with varying degrees of binding of the $3s$ orbital, we vary the well depth. The parameters defining the basis, i.e., the oscillator length in the HO variant and the $\{a, b, R\}$ parameters of the THO basis, have been chosen so as to minimize the single-particle energy of the $3s$ halo state. For a given calculation in either the HO or THO basis, truncation is defined to include *all* single-particle states belonging to $N \leq N_{\max}$ oscillator shells.

The ability of the HO and THO basis expansions to reproduce single-particle energies is illustrated in Fig. 1, which shows the deviation between approximate and exact energies of the $1s$, $2s$, and $3s$ states as a function of $N_{\max}$. The energy of the $3s$ state was assumed in these calculations to be very low: -200 keV (Fig. 1a) and -40 keV (Fig. 1b). As can be seen from the figure, the THO basis offers a systematic improvement over the traditional HO expansion. As an example, $N_{\max}$=20 THO shells are sufficient to reproduce the energy of the $3s$ halo state with an accuracy of 50-60 keV, whereas $N_{\max}\approx$30 is required with the HO basis. For the well-bound $1s$ and $2s$ states, there is also an improvement when using the THO basis. (The low-$N_{\max}$ fluctuations seen in the $1s$ and $2s$ curves reflect the fact that the basis was optimized to the energy of the $3s$ halo state, so that the resulting radial asymptotics is not appropriate for the more deeply-bound orbitals.)

Figures 2-4 compare the exact and approximate wave functions. It is gratifying to see that even with a relatively low number of THO shells the structure of the $3s$ orbital (Figs. 2 and 3) is well reproduced out to 15-18 fm, and the agreement with the exact eigenvector becomes excellent for $N_{\max}$=30. Again, as for the single-particle energies, one needs at least 30 HO shells to obtain results of comparable quality out to 15-18 fm. For well-bound states, such as the $1s$ state at –22.4 MeV shown in Fig. 4, both expansions work equally well: 20 HO or THO shells are sufficient to reproduce the exact result in the physically interesting region.

It is instructive to discuss why so many HO shells are required to reproduce a wave function out to a very large distance. In the HO approximation, the classical radius of an

orbit with principal quantum number N and orbital quantum number ℓ=0 is given by [39]

$$r_{cl} \approx a_{\rm osc}\sqrt{2N}\ . \tag{14}$$

From this we see that the radial information contained in HO wave functions varies quite slowly with the principal quantum number. To build up the large-r dependence in a radial wave function, we must include HO states of very high principal quantum numbers. In contrast, the THO basis has no such restriction on the radial content of its wave functions and convergence can be achieved much more rapidly.

Another rather extreme example is shown in Fig. 5. Here, we consider the single-particle wave function of a 1s state at e=−14 keV. The SQW wave function has a very large spatial extension. In this case, instead of performing the full basis expansion, the *optimized* single-particle 1s HO and THO wave functions were obtained by maximizing their respective overlaps with the exact solution. (In this way one is testing the ability of unperturbed basis states to reproduce the exact wave functions of weakly-bound states.) The corresponding wave functions are plotted in Fig. 5. The THO wave function has a squared overlap with the exact SQW solution of $|\langle{\rm SQW}|{\rm THO}\rangle|^2$=0.994, whereas the HO wave function has a much lower squared overlap of $|\langle{\rm SQW}|{\rm HO}\rangle|^2$=0.877. Clearly, the THO basis with the LST functions (11)-(13) is much better able to reproduce the tail of a halo wave function than the HO basis.

IV. VARIATIONAL CALCULATIONS WITH SKYRME FORCES

In this section, we test whether Slater determinants built up in terms of the single-particle HO and THO wave functions are able to reproduce the results of full self-consistent HF calculations. We follow the energy density functional approach [28,31,40], whereby the total HF energy, taken as an expectation value of the nuclear Hamiltonian over a trial Slater determinant, involves a sum of the Skyrme and Coulomb energies. As usual, the Skyrme energy density is expressed in terms of local nucleon densities, kinetic energy densities, and spin-orbit densities, all defined in terms of the variational single-particle states. The Coulomb energy density, which depends on the local proton density, contains both direct and exchange terms, the latter taken in the Slater approximation. The effective interaction used in these calculations was the Skyrme force SkP [16].

In the HO variational analysis, the energy functional of the SkP Hamiltonian was minimized with respect to two parameters, the proton and neutron harmonic-oscillator lengths. In the THO analysis, the energy minimization involved the six parameters that define the LST functions for neutrons $\{a_n, b_n, R_n\}$ and protons $\{a_p, b_p, R_p\}$. The calculations were carried out for three spherical doubly-magic nuclei, ^{16}O, ^{40}Ca, and ^{208}Pb.

Table I contains the results for ground-state binding energies and proton and neutron rms radii. As expected, the binding energies based on THO Slater determinants are lower than those based on the HO. The HF binding energies are of course lower than those based on either the HO or THO Slater determinants because of the self-consistent nature of HF calculations (the HF state is the optimal Slater determinant for a given Hamiltonian). In all cases considered, the THO binding energies are within 1.1% of the HF results, while the HO results deviate up to 5% for heavy nuclei. For neutron and proton rms radii, the THO results

agree very well with the self-consistent HF values, whereas the HO results systematically overestimate them.

Table II compares the neutron single-particle energies that resulted from the restricted HO and THO variational calculations with those from the self-consistent HF calculations. The restricted calculations give a rather good approximation to the self-consistent single-particle energies. In general, the best agreement is obtained for the high-ℓ states where the tail of the wave function plays little role. The largest deviations are seen for s and p states.

Finally, the neutron and proton density distributions resulting from the various calculations are compared in Fig. 6. There is excellent agreement between the THO and self-consistent HF densities in the surface region. In contrast, the incorrect asymptotic behavior of HO wave functions leads to significant deviations [41]. The THO densities differ most significantly from the HF results at small values of r. However, since the densities are weighted by r^2 in calculations of expectation values, the main contribution to global nuclear characteristics such as energies and rms radii comes from the surface region.

V. SUMMARY AND CONCLUSIONS

In this paper, we have explored a new class of single-particle basis states obtained by a local-scale point transformation (LST) of harmonic oscillator states. We focussed special attention on the asymptotic properties of these states (called THO states), to see whether they might be useful in the description of weakly-bound nuclear systems, including those with a halo structure.

Following a comprehensive summary of the LST formalism and its use in building the THO basis, we discussed two applications of this new basis. The first concerned the description of sub-threshold (halo) states. We showed that the THO basis is greatly superior to the usual HO basis in reproducing the properties of such weakly-bound states. We then discussed the use of this basis in restricted HF calculations. Once again, the clear superiority of the THO basis to the ordinary HO basis was demonstrated, even for normal well-bound nuclei. Most importantly, the optimal THO basis that emerged from the restricted HF calculations provided an excellent reproduction of nuclear surface properties.

The analysis presented in this paper should be viewed as a starting point for future investigations. One potentially interesting application of the THO basis is in the context of nuclear shell-model studies. The fact that the THO basis expansion technique and the THO variational procedure accurately reproduce nuclear properties in the surface region suggests that the new basis can be very useful when studying those nuclear properties that depend on the asymptotic behavior of the radial form-factor, and also for microscopic calculations of the effective interactions for weakly bound systems [42]. Some of the simplicity inherent in the use of HO wave functions in such studies will be lost, however. Calculations of G-matrix elements, for example, benefit greatly from the ease of transforming harmonic oscillator product wave functions into relative and center-of-mass coordinates, and this would be lost in the THO basis. On the other hand, it should be still much easier to carry out calculations in this basis than in a basis generated by numerical solution of the single-particle Schrödinger equation.

Another interesting avenue for future exploration concerns the use of the THO basis in HFB or RHB calculations of weakly-bound nuclei where other traditional methods (e.g.,

HF+BCS) cannot be used [16,17]. The fact that with a rather modest number of basis THO states one can reproduce the properties of spatially extended states suggests that the traditional method of solving the HFB equations, based on basis expansion, can be revitalized by using the THO basis. This way of solving the HFB problem (both in the spherical and deformed cases) can be an interesting alternative to algorithms based on coordinate-space methods [21–23].

Finally, the THO states that arise variationally can be used as approximations to the self-consistent canonical states of HFB. Recently, the variational method based on the energy density formalism was generalized to the HFB case [43]. In that work, the authors employed the basis proposed by Ginocchio [44] in the description of semi-magic nuclei. Despite the successes achieved in those calculations and in earlier restricted HF calculations for doubly-magic nuclei [45], there are several features of the Ginocchio potential that make its more detailed use problematical. First, since the centrifugal term in the Ginocchio potential is not treated properly, the resulting wave functions with $\ell>0$ do not have proper asymptotic behavior. Second, since the Ginocchio potential is finite, its bound eigenvectors do not form a closed set, and the use of the continuum wave functions is necessary (see recent Ref. [46]). In this context, the discrete THO basis would appear to be more useful.

ACKNOWLEDGMENTS

Useful discussions with Jacek Dobaczewski are gratefully acknowledged. This research was supported in part by the Bulgarian National Foundation for Scientific Research under contract No. Φ-527, the U.S. Department of Energy under Contract Nos. DE-FG02-96ER40963 (University of Tennessee), DE-FG05-87ER40361 (Joint Institute for Heavy Ion Research), DE-AC05-96OR22464 with Lockheed Martin Energy Research Corp. (Oak Ridge National Laboratory), and by the U. S. National Science Foundation under Grant Nos. PHY-9600445 and INT-9722810.

REFERENCES

[1] U. Fano, Phys. Rev. **124**, 1866 (1961).
[2] W. Glöckle, J. Hufner, and H.A. Weidenmueller, Nucl. Phys. **A90**, 481 (1967).
[3] R.J. Philpott, Fizika **9**, suppl. 3, 21 (1977).
[4] M. Micklinghoff, Nucl. Phys. **A295**, 228 (1978).
[5] D. Halderson and R.J. Philpott, Nucl. Phys. **A345**, 141 (1980).
[6] W. Iskra and I. Rotter, Phys. Rev. **C44**, 721 (1991).
[7] K. Bennaceur, F. Nowacki, J. Okolowicz, and M. Płoszajczak, nucl-th/9802054.
[8] J.S. Vaagen, B.S. Nilsson, J. Bang, and R.M. Ibarra, Nucl. Phys. **A319**, 143 (1979).
[9] G. Rawitscher, Phys. Rev. **C25**, 2196 (1982).
[10] W.J. Romo, Nucl. Phys. **A191**, 65 (1972).
[11] T. Berggren, Nucl. Phys. **A109**, 265 (1968).
[12] T. Vertse, P. Curutchet, and R.J. Liotta, Lecture Notes in Physics **325** (Springer Verlag, Berlin 1987), p. 179.
[13] P. Lind, R.J. Liotta, E. Maglione, and T. Vertse, Z. Phys. **A347**, 231 (1994).
[14] T. Berggren, Phys. Lett. **B373**, 1 (1996).
[15] S. Fortunato, A. Insolia, R.J. Liotta, and T. Vertse, Phys. Rev. **C54**, 3279 (1997).
[16] J. Dobaczewski, H. Flocard and J. Treiner, Nucl. Phys. **A422**, 103 (1984).
[17] J. Dobaczewski, W. Nazarewicz, T.R. Werner, J.-F. Berger, C.R. Chinn, and J. Dechargé, Phys. Rev. **C53**, 2809 (1996).
[18] D.L. Tubbs and S.E. Koonin, Astrophys. J. **232**, L59 (1979).
[19] A.K. Kerman and S. Levit, Phys. Rev. **C24**, 1029 (1981).
[20] D.R. Dean and U. Mosel, Z. Phys. **A322**, 647 (1985).
[21] J. Terasaki, P.-H. Heenen, H. Flocard, and P. Bonche, Nucl. Phys. **A600**, 371 (1996).
[22] P.-G. Reinhard, M. Bender, K. Rutz, and J.A. Maruhn, Preprint nucl-th/9705054.
[23] W. Poschl, D. Vretenar, P. Ring, Comp. Phys. Commun. **103**, 217 (1997).
[24] K. Heyde, *The Nuclear Shell Model* (Springer Verlag, Berlin, 1990).
[25] *Group Theory in Physics*, Proc. Int. Symp. Cocoyoc, Mexico; 3-7 June 1991, AIP Conference Proceedings, no. 266.
[26] I. Talmi, *Simple Models of Complex Nuclei. The Shell Model and Interacting Boson Model*, (Harwood, 1993).
[27] I.Zh. Petkov and M.V. Stoitsov, Compt. Rend. Bulg. Acad. Sci. **34**, 1651 (1981); Theor. Math. Phys. **55**, 584 (1983); Sov. J. Nucl. Phys., **37** 692 (1983).
[28] S.S. Dimitrova, I.Zh. Petkov, and M.V. Stoitsov, Z. Phys., **A325**, 15 (1986).
[29] M.V. Stoitsov and I.Zh. Petkov, Ann. Phys. (NY) **184**, 121 (1988).
[30] S.S. Dimitrova, I.Zh. Petkov, and M.V. Stoitsov, Nucl. Phys. **A485**, 233 (1988).
[31] I.Zh. Petkov and M.V. Stoitsov, *Nuclear Density Functional Theory*, Oxford Studies in Physics, (Clarendon Press, Oxford, 1991).
[32] J. Friedrich, N. Voegler, and P.-G. Reinhard, Nucl. Phys. **A459**, 10 (1986).
[33] A. Mueller and B. Sherril, Annu. Rev. Nucl. Part. Sci. **43**, 529 (1993).
[34] K. Riisager, Rev. Mod. Phys. **66**, 1105 (1994).
[35] P.G. Hansen, A.S. Jensen, B. Jonson, Annu. Rev. Nucl. Part. Phys. **45**, 591 (1995).
[36] I. Tanihata, Jour. of Phys. G **22**, 157 (1996).
[37] K. Riisager, A.S. Jensen, and P. Møller, Nucl. Phys. **A548**, 393 (1992).
[38] T. Misu, W. Nazarewicz, and S. Åberg, Nucl. Phys. **A614**, 44 (1997).

[39] A. Bohr and B.R. Mottelson, Nuclear Structure, vol. 1 (W.A. Benjamin, New York, 1969).
[40] M. Brack, C. Guet and H.-B. Håkansson, Phys. Rep. **123**, 275 (1985).
[41] R. Bengtsson, J. Dudek, W. Nazarewicz and P. Olanders, Phys. Scr. **39** (1989) 196.
[42] T.T. Kuo, F. Krmpotić, and Y. Tzeng, Phys. Rev. Lett. **78**, 2708 (1997).
[43] M.V. Stoitsov and S. Pittel, to be published.
[44] J.N. Ginocchio, Ann. Phys. (NY) **159**, 467 (1985).
[45] M.V. Stoitsov, S.S. Dimitrova, S. Pittel, P. Van Isacker, and A. Frank, Phys. Lett. **B415** (1997) 1.
[46] K. Bennaceur *et al.*, to be published.

TABLES

TABLE I. Total binding energies and neutron and proton rms radii obtained using HO and THO Slater determinants and from self-consistent HF calculations for the spherical doubly-magic nuclei ^{16}O, ^{40}Ca, and ^{208}Pb.

	^{16}O			^{40}Ca			^{208}Pb		
	HO	THO	HF	HO	THO	HF	HO	THO	HF
E (MeV)	-125.9	-126.2	-127.6	-339.1	-340.9	-343.3	-1565.5	-1621.8	-1636.5
$\langle r_p \rangle_{\rm rms}$ (fm)	2.73	2.73	2.73	3.46	3.45	3.45	5.49	5.47	5.47
$\langle r_n \rangle_{\rm rms}$ (fm)	2.71	2.71	2.70	3.42	3.40	3.40	5.64	5.61	5.61

TABLE II. Spherical single-neutron energies (in MeV) obtained using HO and THO Slater determinants and from self-consistent HF calculations for the spherical doubly-magic nuclei ^{16}O, ^{40}Ca, and ^{208}Pb.

	^{16}O			^{40}Ca			^{208}Pb		
nlj	HO	THO	HF	HO	THO	HF	HO	THO	HF
$1s_{1/2}$	-29.0	-29.2	-29.0	-36.4	-37.1	-37.4	-37.1	-39.0	-40.0
$1p_{3/2}$	-17.9	-17.9	-18.3	-29.0	-29.1	-28.9	-34.8	-35.6	-36.4
$1p_{1/2}$	-13.5	-13.6	-13.6	-25.5	-25.5	-25.8	-33.3	-35.1	-35.8
$1d_{5/2}$				-19.6	-19.6	-19.7	-31.3	-31.6	-31.9
$2s_{1/2}$				-14.9	-15.5	-16.4	-28.7	-29.8	-29.2
$1d_{3/2}$				-14.5	-14.5	-14.4	-29.0	-30.4	-30.6
$1f_{7/2}$							-26.7	-26.7	-26.9
$2p_{3/2}$							-23.2	-23.8	-23.3
$1f_{5/2}$							-23.5	-24.5	-24.5
$2p_{1/2}$							-21.7	-22.7	-22.4
$1g_{9/2}$							-21.1	-21.1	-21.3
$2d_{5/2}$							-17.1	-17.5	-17.2
$1g_{7/2}$							-17.0	-17.6	-17.6
$3s_{1/2}$							-15.0	-15.8	-15.5
$2d_{3/2}$							-14.6	-15.5	-15.6
$1h_{11/2}$							-14.8	-15.0	-15.3
$2f_{7/2}$							-11.0	-11.3	-10.9
$1h_{9/2}$							-9.7	-10.0	-10.1
$1i_{13/2}$							-8.0	-8.5	-8.8
$3p_{3/2}$							-9.0	-9.5	-8.9
$2f_{5/2}$							-7.8	-8.5	-8.6
$3p_{1/2}$							-7.7	-8.4	-8.1

FIGURES

FIG. 1. Deviation between approximate energies based on the basis expansion method and exact energies of the $1s$, $2s$, and $3s$ states of the SQW Hamiltonian as a function of the number of HO quanta included in the basis, $N_{\max}$. The solid lines are the results obtained when expanding in a HO basis; the dotted lines are the results obtained using the THO basis. The radius of the well was taken to be R_0=7.11 fm. The different binding energies of the $3s$ halo orbital, −200 keV (a) and −40 keV (b), were achieved by changing the well depth.

FIG. 2. Exact (dots) and approximate (lines) wave functions of the $3s$ halo state at e=−200 keV as a function of r. The approximate wave functions were obtained by means of the basis expansion method (HO, left panel; THO, right panel) in $N_{\max}$=12, 20, 30, and 40 HO (THO) shells.

FIG. 3. Same as in Fig. 2 but for the wave functions of the $3s$ halo state at e=−40 keV and for $N_{\max}$=12, 20, 30, and 60 HO (THO) shells.

FIG. 4. Same as in Fig. 2 but for the wave functions of the well-bound $1s$ state at e=−22.4 MeV.

FIG. 5. The wave function of a $1s$ SQW eigenstate at e=–14 keV (SQW, solid line). The HO (dotted line) and THO (dashed line) $1s$ wave functions were determined by maximizing their overlap with the SQW state. The asymptotic behavior (in logarithmic scale) is shown in the insert.

FIG. 6. Local one body densities for ^{16}O, ^{40}Ca, and ^{208}Pb calculated in the self-consistent HF approach (solid line) compared with those obtained in restricted variational calculations using as trial wave functions Slater determinants built from HO (dotted line) and THO (dashed line) single-particle orbitals. All calculations utilized the same SkP effective interation.

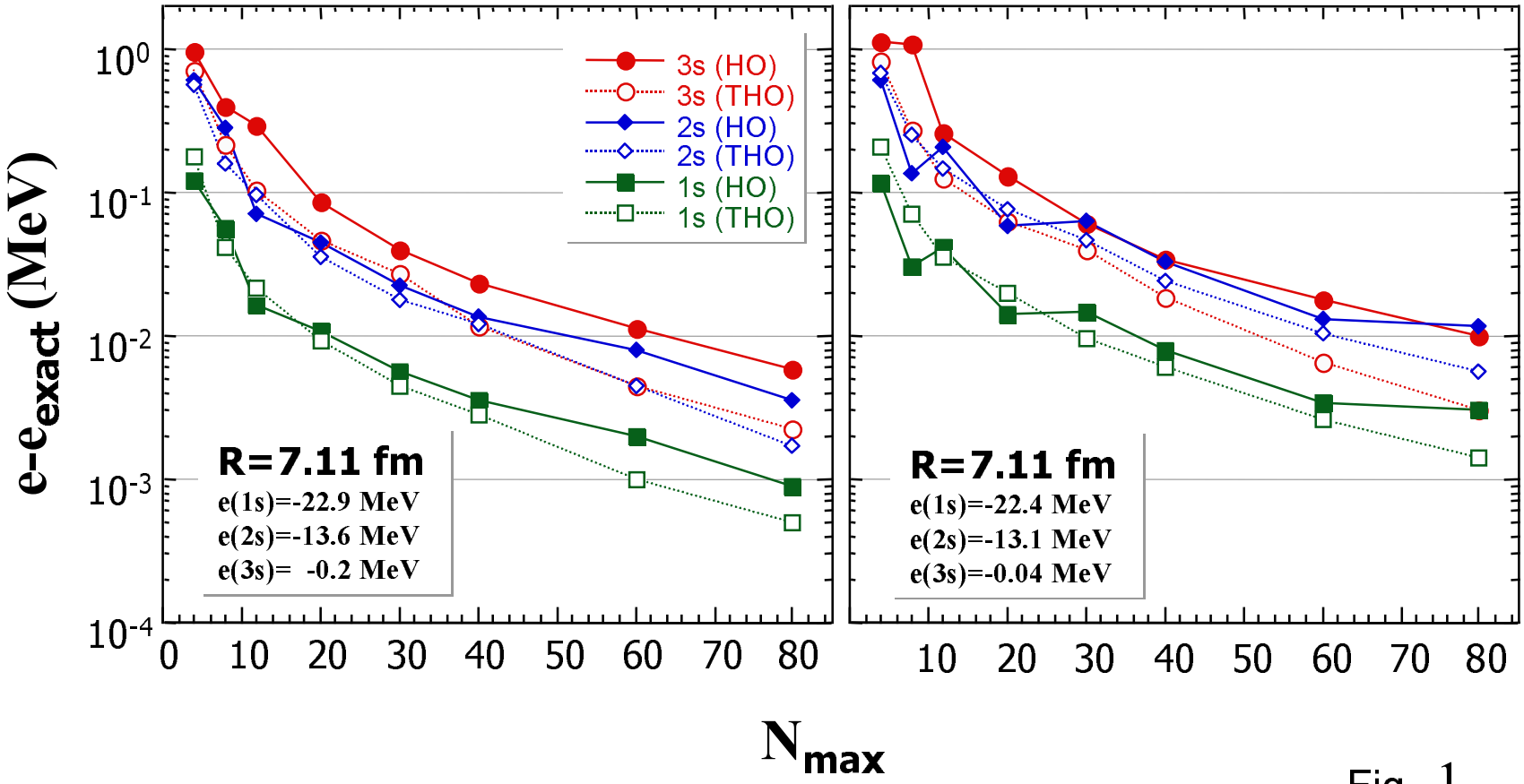
e-e_exact (MeV)
10^0
10^-1
10^-2
10^-3
10^-4
0
10
20
30
40
50
60
70
80
3s (HO)
3s (THO)
2s (HO)
2s (THO)
1s (HO)
1s (THO)
R=7.11 fm
e(1s)=-22.9 MeV
e(2s)=-13.6 MeV
e(3s)= -0.2 MeV
R=7.11 fm
e(1s)=-22.4 MeV
e(2s)=-13.1 MeV
e(3s)=-0.04 MeV
N_max

Fig. 1

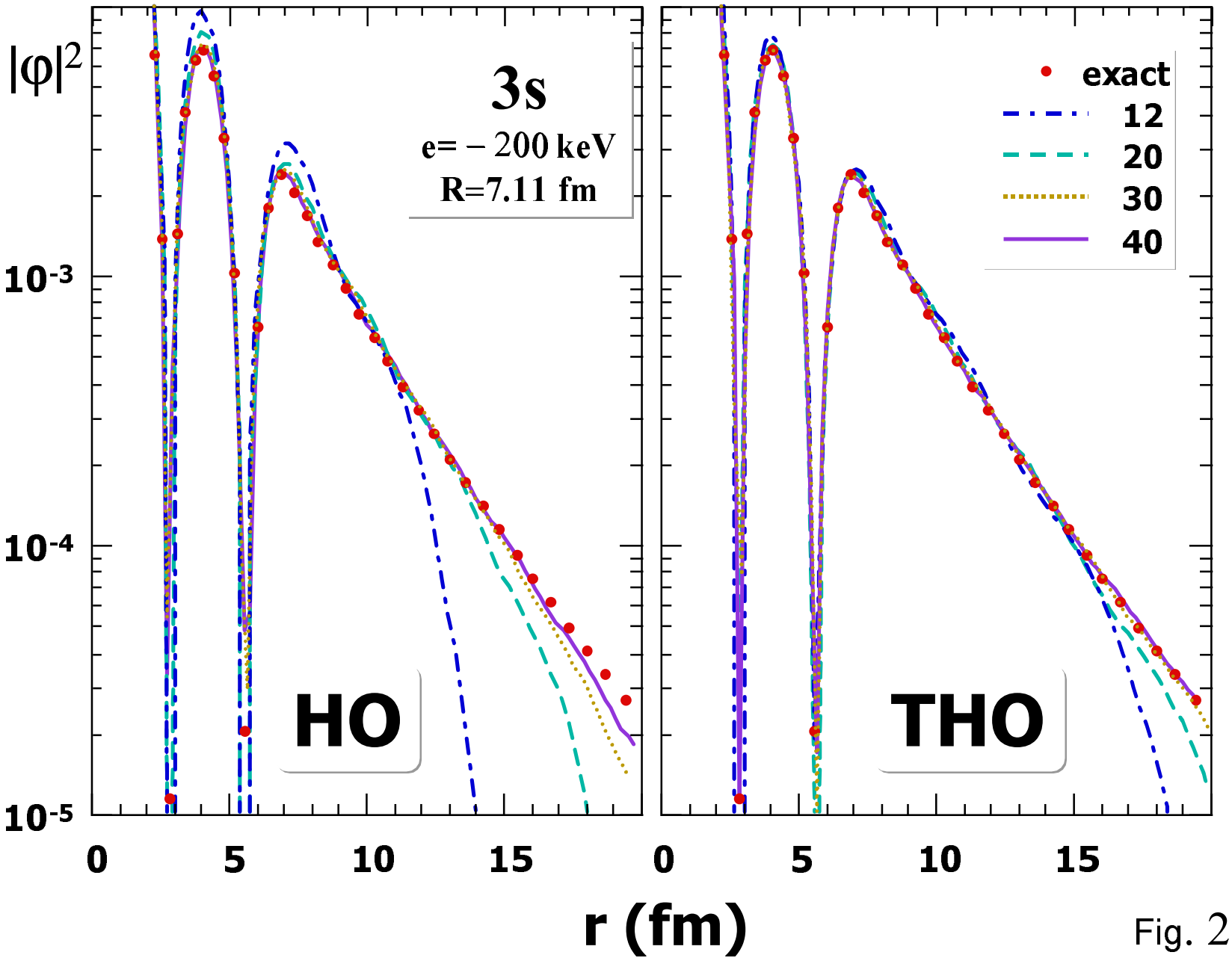
|φ|²
3s
e= – 200 keV
R=7.11 fm
exact
12
20
30
40
HO
THO
10⁻³
10⁻⁴
10⁻⁵
0
5
10
15
0
5
10
15
r (fm)

Fig. 2

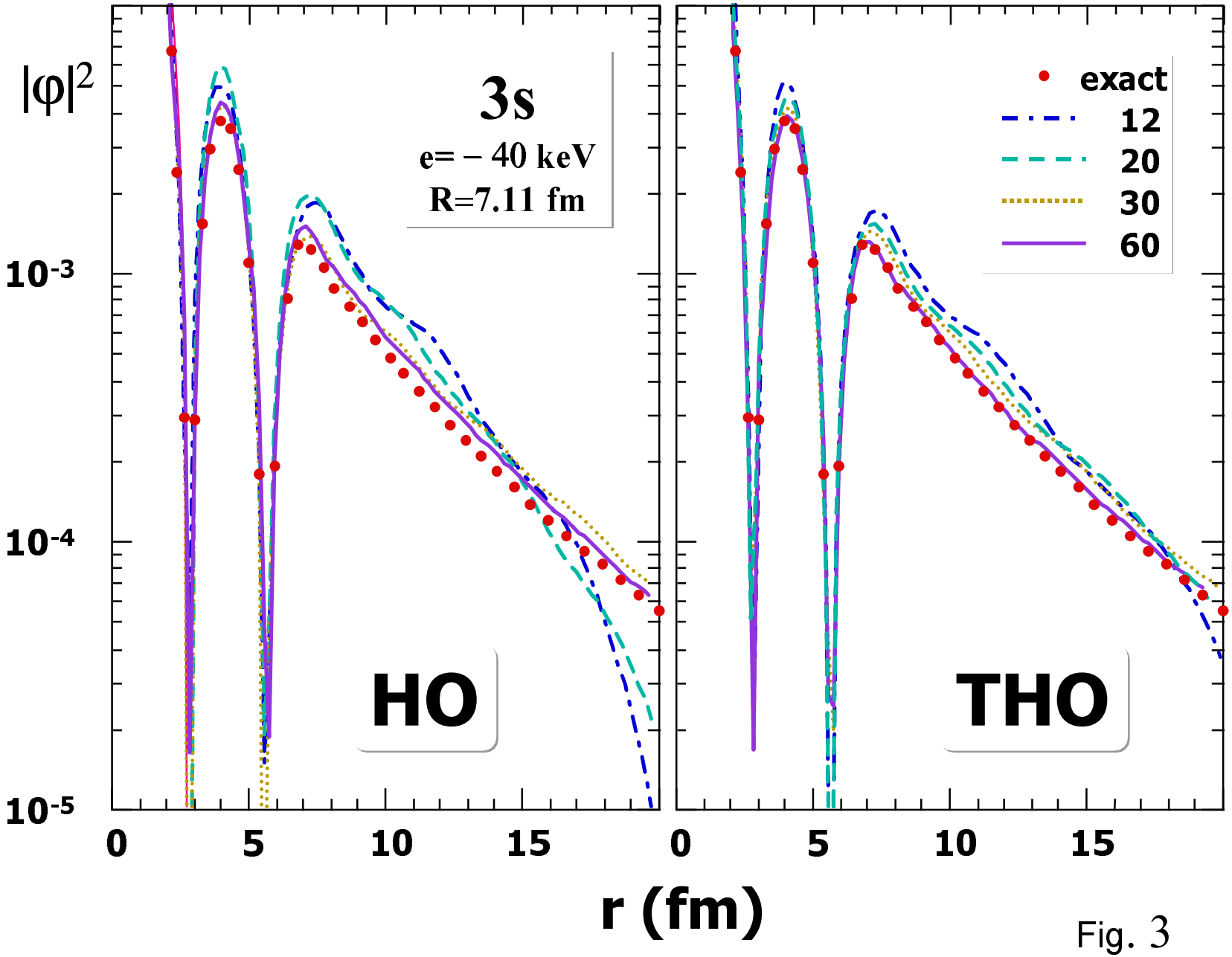
|φ|²
3s
e= – 40 keV
R=7.11 fm
exact
12
20
30
60
HO
THO
10-3
10-4
10-5
0
5
10
15
0
5
10
15
r (fm)

Fig. 3

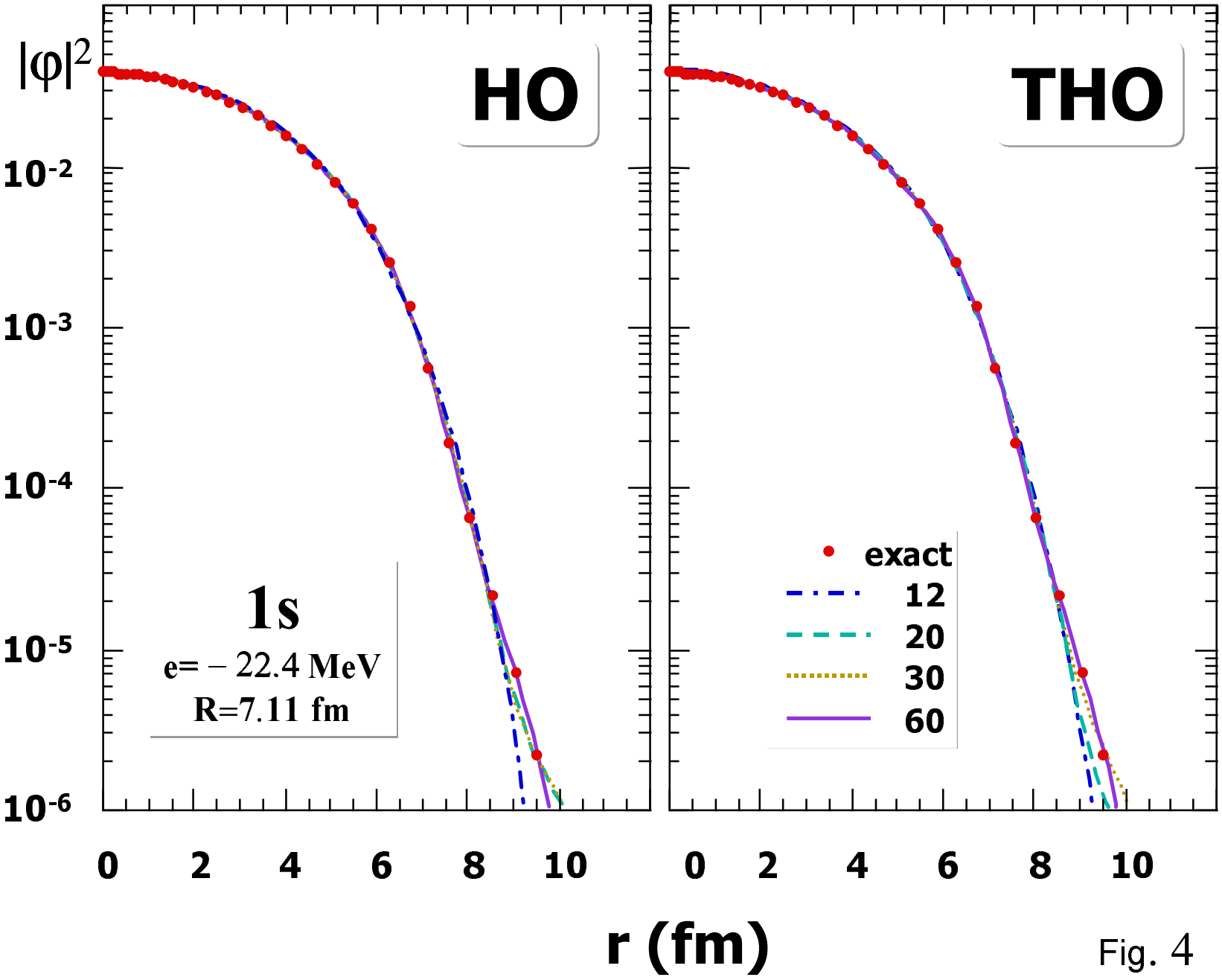
|φ|²
HO
THO
10⁻²
10⁻³
10⁻⁴
10⁻⁵
10⁻⁶
1s
e= – 22.4 MeV
R=7.11 fm
exact
12
20
30
60
0
2
4
6
8
10
r (fm)

Fig. 4

fig. 5

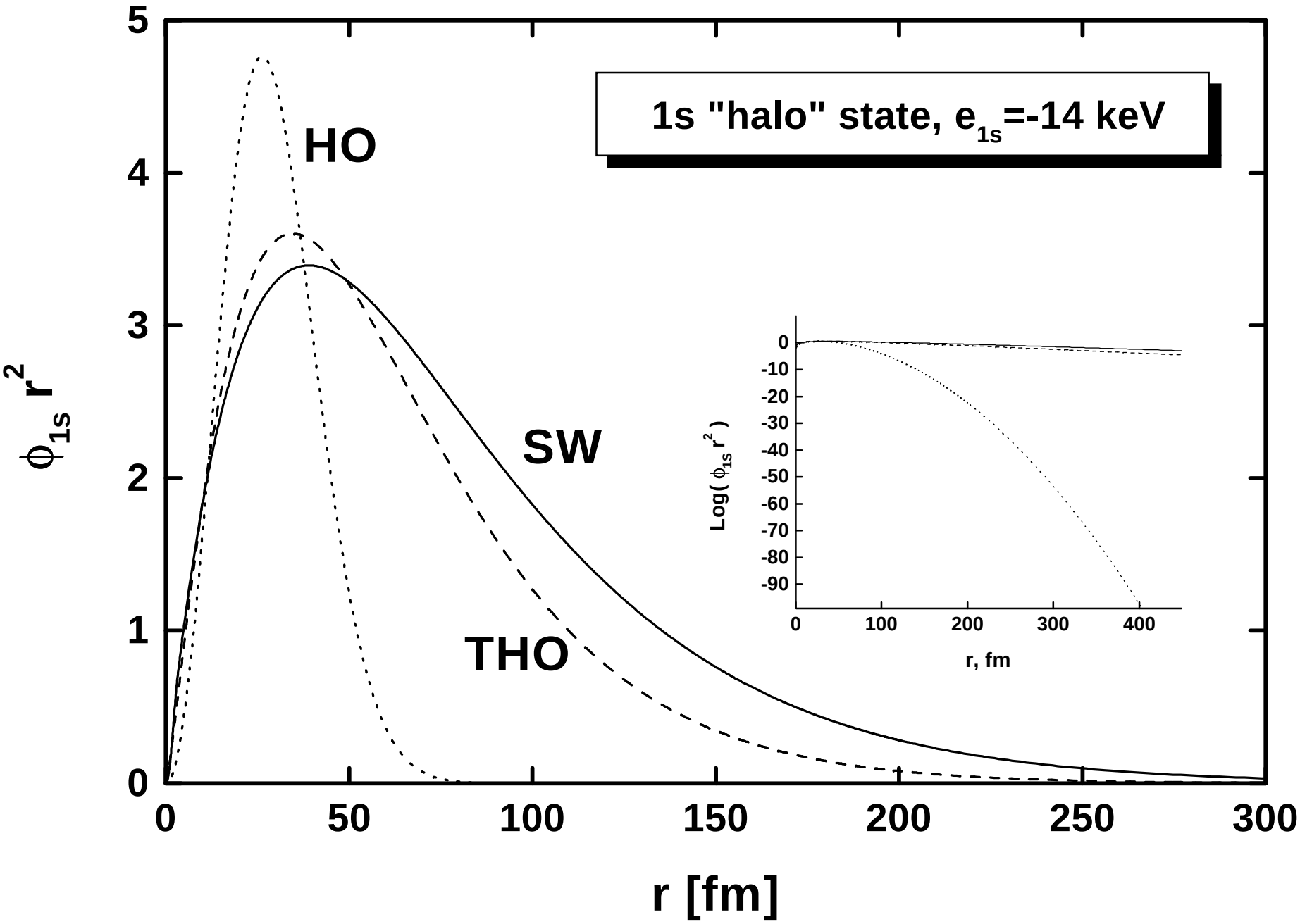

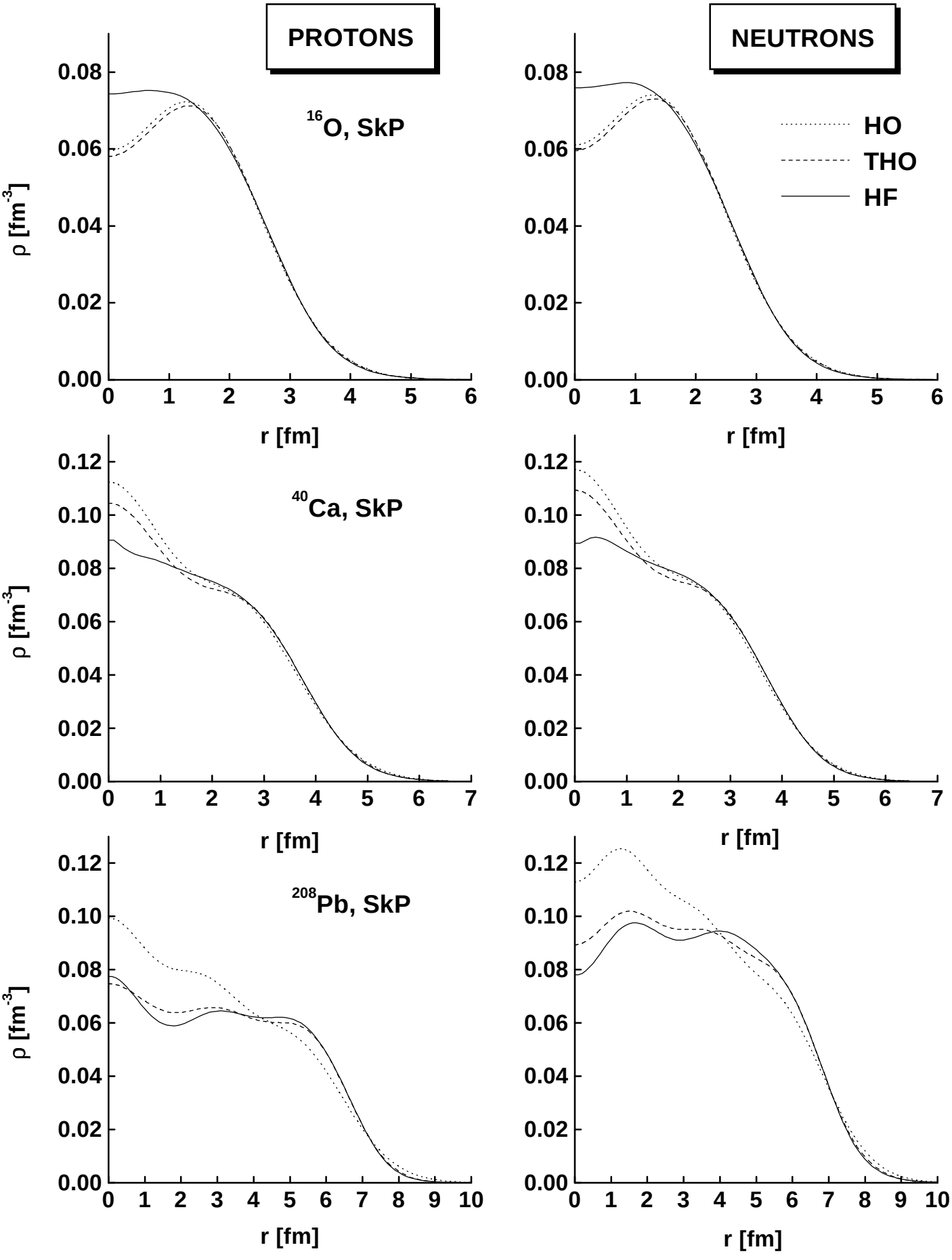
PROTONS
NEUTRONS
^{16}O, SkP
^{40}Ca, SkP
^{208}Pb, SkP
HO
THO
HF
ρ [fm^{-3}]
r [fm]

fig. 6